The Astrophysical Journal, 615:L25–L28, 2004 November 1

AN UNVEILING EVENT IN THE TYPE 2 ACTIVE GALACTIC NUCLEUS NGC 4388: A CHALLENGE FOR A PARSEC-SCALE ABSORBER

Martin Elvis,[1] G. Risaliti,[1,2] F. Nicastro,[1] J. M. Miller,[1,3] F. Fiore,[4] and S. Puccetti[4]
Received 2004 March 19; accepted 2004 July 14; published 2004 October 4

ABSTRACT

We present two *Rossi X-Ray Timing Explorer* (*RXTE*) Proportional Counter Array (PCA) observations of the type 2 Seyfert galaxy NGC 4388 caught in an unusual low X-ray absorption state. The observations were triggered by a detection in the 1.5–3 keV band of the *RXTE* all-sky monitor. NGC 4388 was found at a somewhat high continuum level [f(2–10 keV) $= 8 \times 10^{-11}$ ergs cm^{-2} s^{-1}] and with a column density $N_{\rm H} \sim 3 \times 10^{22}$ cm^{-2}, a factor of ∼10 lower than normal. The second PCA observation, 4 hr later, gave $N_{\rm H} < 2 \times 10^{21}$ cm^{-2} indicating, at the 3.1 σ level, variability so rapid it puts the absorber on a few 100 Schwarzschild radii scale, similar to the broad emission line region or smaller. This small scale creates difficulties for the parsec-scale obscuring torus paradigm of unified schemes for type 1 and type 2 active galactic nuclei.

Subject headings: galaxies: active — galaxies: individual (NGC 4388) — galaxies: Seyfert — X-rays: galaxies

Online material: color figures

1. INTRODUCTION

Optically NGC 4388 is a classical type 2 Seyfert galaxy (Huchra et al. 1982) with permitted and forbidden emission lines of the same width (Khachikian & Weedman 1974). There is abundant evidence that many, and perhaps all, type 2 active galactic nuclei (AGNs) are normal type 1 AGNs with both the characteristic broad emission lines and the optical–to–X-ray continuum obscured by a flattened torus of absorbing gas and dust (e.g., Mulchaey et al. 1994). This is the basis of the unified scheme for AGNs (Antonucci 1993; Urry & Padovani 1995). NGC 4388 has been detected in X-rays for over 20 yr (Table 1) and has always shown a column density $N_{\rm H} = (2\text{–}5) \times 10^{23}$ cm^{-2}.

The most common form of the unified scheme locates this absorption in a dusty torus at parsec distances from the central continuum (Krolik & Begelman 1988; Pier & Krolik 1992, 1993). However, Risaliti et al. (2002) found that 23/24 X-ray–absorbed AGNs (10^{22} cm^{-2} $< N_{\rm H} < 3 \times 10^{23}$ cm^{-2}) showed $N_{\rm H}$ variability by a factor of 2–3. The best-studied objects varied on the shortest accessible timescale of months, which is rather fast to be due to Keplerian motion at parsec radii and so raises questions about the nature of the obscuring torus.

Risaliti et al. suggested an alternative location in the cool outer parts of an accretion disk wind, echoing the model of Kartje et al. (1999), who predicted just such a torus. This location predicts much faster $N_{\rm H}$ variability, down to a timescale of days. In a simple model of Poisson variations in the number of obscuring clouds, N_c, the amplitude of variability found by Risaliti et al. implies $N_c \sim 5$–10. In this case 0.1%–1% of the time $N_c = 0$ and, in the unified scheme, the central type 1 nucleus would then be unveiled.

The *Rossi X-Ray Timing Explorer* (*RXTE*; Swank et al. 1998) all-sky monitor (ASM; Remillard & Levine 1997) is just sensitive enough to detect such low-energy "unveiling events." We thus began a Target of Opportunity program with *RXTE* to obtain snapshot Proportional Counter Array (PCA; Swank 1998) spectra of type 2 AGNs showing signs of a low-energy detection in the *RXTE* ASM. Here we report the detection of a low $N_{\rm H}$ unveiling event in NGC 4388.

2. OBSERVATIONS AND DATA REDUCTION

We monitored NGC 4388 with the *RXTE* ASM to search for detections in the soft 1.5–3 keV X-ray channel ("a"). Normally NGC 4388 has a flux of $\sim 4 \times 10^{-13}$ ergs cm^{-2} s^{-1} in this band (Forman et al. 1979), while a detection requires a flux some 250 times larger ($\sim 1 \times 10^{-10}$ ergs cm^{-2} s^{-1}). Simply removing the large absorbing $N_{\rm H}$ [$\sim (2\text{–}5) \times 10^{23}$cm^{-2}] would increase the observed flux to $\sim 4 \times 10^{-11}$ ergs cm^{-2} s^{-1}, a factor of 100, so that only a modest additional factor 2–3 increase in the emitted continuum would be needed to put NGC 4388 over the threshold for ASM detection. By contrast, an increase in the emitted continuum flux by a factor greater than 100 would be unprecedented among the well-studied type 1 AGNs, where factors of a few to ∼10 variation are seen (Markowitz et al. 2003). Hence an ASM "a" band detection is a good indicator of a low $N_{\rm H}$ event. A triggering event of this type occurred on 2003 May 9 (Fig. 1), shortly after another one (which is visible on the left side of Fig. 1). One day after the ASM trigger, NGC 4388 was observed twice with the *RXTE* PCA, for 1.9 and 6.2 ks, with a 4 hr gap between the two observations (Fig. 1).

We only consider data from PCU-2 for this analysis, as this is the best-calibrated Proportional Counter Unit (PCU) in the *RXTE*/PCA.[5] Data reduction tools from LHEASOFT version 5.2 were used to screen and prepare the event files and spectra. Data were taken in "Standard 2" mode, which provides coverage of the full PCA bandpass (2–60 keV) every 16 s. Only data from the top Xe-filled gas layer in PCU-2 were used to make the source and background spectra, as this gas layer has the lowest background. The standard *RXTE* "Good Time Interval" filtering was applied to the data. For the nonimaging PCA, accurate background subtraction is crucial for faint sources such as NGC 4388. The background spectra were made using the tool PCABACKEST using the latest "faint source" background model (pca_bkgd_cmfaintl7_e5vv20031123.mdl,

[1] Harvard-Smithsonian Center for Astrophysics, 60 Garden Street, Cambridge, MA 02138; elvis@cfa.harvard.edu.
[2] INAF–Osservatorio di Arcetri, Largo Enrico Fermi 5, Florence I-50125, Italy.
[3] NSF Astronomy and Astrophysics Postdoctoral Fellow.
[4] INAF–Osservatorio di Roma, Sede di Monteporzio Catone, Via di Frascati, 33, Rome I-00040, Italy.

[5] See http://lheawww.gsfc.nasa.gov/users/keith/bkgd_status/status.html and http://heasarc.gsfc.nasa.gov/listserv/grodis/msg00066.html.

TABLE 1
X-Ray Observations of NGC 4388

Instrument	N_H[a]	Γ	E_{Fe}[b]	σ_{Fe}[c]	EW_{Fe}[d]	F[e]	L[f]	Observation Date	Reference
SL2-XRT	$2.1^{+2.8}_{-1.4}$	$1.9^{+0.9}_{-0.5}$	…	…	…	2.1	3.5	1985 Jul 29	1
ASCA-1	$3.15^{+1.1}_{-1.0}$	$1.32^{+0.77}_{-0.74}$	$6.49^{+0.09}_{-0.09}$	150^{+160}_{-130}	750^{+420}_{-300}	1.3	1.5	1994 Jul 04	2
ASCA-2	$3.34^{+1.0}_{-0.9}$	$1.47^{+0.57}_{-0.57}$	$6.47^{+0.07}_{-0.07}$	<200	700^{+320}_{-250}	0.64	0.7	1995 Jun 21	2
BeppoSAX-1	$3.80^{+0.2}_{-0.4}$	$1.58^{+0.08}_{-0.22}$	$6.46^{+0.07}_{-0.10}$	<230	233^{+115}_{-35}	2.5	3.5	1999 Jan 09	3
BeppoSAX-2	$4.80^{+1.8}_{-0.8}$	$1.47^{+0.04}_{-0.41}$	$6.38^{+0.05}_{-0.06}$	<120	525^{+115}_{-112}	0.94	1.4	2000 Jan 03	3
Chandra	$3.50^{+0.4}_{-0.3}$	1.8	$6.36^{+0.02}_{-0.02}$	<230	440^{+90}_{-90}	0.36	0.6	2001 Jun 08	4
Chandra-0	$2.50^{+0.2}_{-0.1}$	$1.25^{+0.14}_{-0.28}$	$6.36^{+0.03}_{-0.03}$	<130	165^{+60}_{-60}	2.9	2.8	2002 Mar 05	5
XMM-1	$1.70^{+0.12}_{-0.15}$	$0.91^{+0.10}_{-0.37}$	$6.41^{+0.02}_{-0.02}$	<77	503^{+70}_{-60}	0.77	0.7	2002 Jul 07	5
XMM-2	$2.61^{+0.06}_{-0.06}$	$1.46^{+0.04}_{-0.05}$	$6.44^{+0.02}_{-0.02}$	73^{+20}_{-20}	204^{+24}_{-26}	2.0	2.2	2002 Dec 12	5
RXTE/PCA-1	$0.52^{+0.25}_{-0.24}$	$0.99^{+0.11}_{-0.11}$	$6.34^{+0.11}_{-0.11}$	<380	503^{+138}_{-100}	7.2	4.0	2003 May 10	5
RXTE/PCA-2	<0.09	$0.86^{+0.07}_{-0.03}$	$6.32^{+0.10}_{-0.09}$	390^{+160}_{-190}	570^{+114}_{-100}	6.1	2.9	2003 May 10	5

[a] Absorbing column density in units of 10^{23} cm^{-2}.
[b] Peak energy of the iron Kα line in units of keV.
[c] Width of the iron line in units of eV.
[d] EW of the iron line in units of eV.
[e] Observed 2–10 keV flux in units of 10^{-11} ergs s^{-1} cm^{-2}.
[f] Intrinsic 2–10 keV luminosity in units of 10^{42} ergs s^{-1} cm^{-2} (assuming a Virgo Cluster location at 20 Mpc).
References.—(1) Hanson et al. 1990; (2) Forster et al. 1999; (3) Risaliti 2002; (4) Iwasawa et al. 2003; (5) this work.

updated by *RXTE* in 2003 November). PCABACKEST calculates the predicted (dominant) particle background every 16 s and so tracks the variation of the background around the orbit, thus taking into account the different backgrounds in these two short observations. Redistribution matrix files and ancillary response files were made and combined into a single instrumental response file using PCARSP.[6]

We added 0.6% systematic errors to our spectra using GRPPHA, as we find that in many instances acceptable fits to the Crab can be obtained with 0.6% systematic errors. However, Poisson errors of 5%–10% are dominant. The lowest channels in each of the PCUs routinely reveal strong deviations likely due to calibration uncertainties; in addition, the calibration of the PCUs is more uncertain above approximately 25 keV, and the spectra of faint sources such as NGC 4388 become background-dominated in this regime. In fitting the spectra, then, we ignored the energy range below 3 keV (channels 1–4) and above 20.0 keV.

The PCA X-ray spectra are shown in Figure 2 (*top*), where they are compared with a *Chandra* observation performed 14 months earlier. Figure 2 (*top*) shows that most of the variation is at low energies, less than 5 keV. In Figure 2 (*bottom*) we show the ratio between the two *RXTE* spectra, which indicates that the cutoff in the spectra at low energies is due to a difference in N_H.

To fit the PCA spectra we used XSPEC version 11.3. A model comprising a power law of slope Γ, absorbed by a zero redshift N_H, with a superposed emission line near the 6.4 keV Fe-K line energy, was fitted to the two PCA data sets and gave good χ^2 (30/34 degrees of freedom for PCA-1 and 25/34 degrees of freedom for PCA-2). The low redshift of NGC 4388 (2535 km s^{-1}; Huchra et al. 1982) is indistinguishable from zero with the PCA. The

[6] See http://heasarc.gsfc.nasa.gov/docs/software/lheasoft.

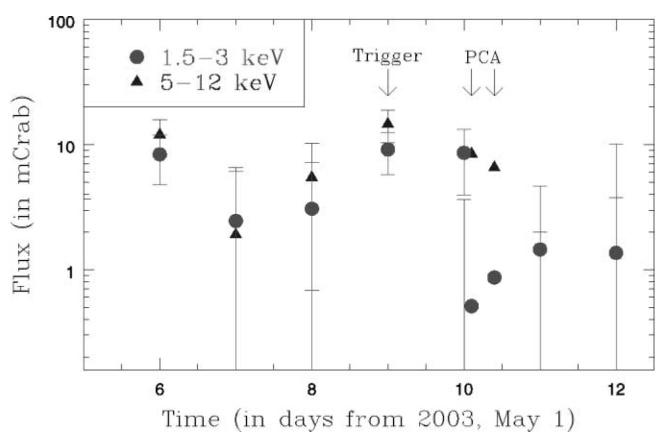

Fig. 1.—*RXTE* ASM light curve of NGC 4388 that triggered the pointed observations. The "a" (1.5–3 keV) band fluxes are shown as circles, and the "c" (5–12 keV) band fluxes are shown as triangles. The triggering data points are marked. The two pointed PCA fluxes in the same bands are also shown. The error bars on the PCA measurements are smaller than the points. [*See the electronic edition of the Journal for a color version of this figure.*]

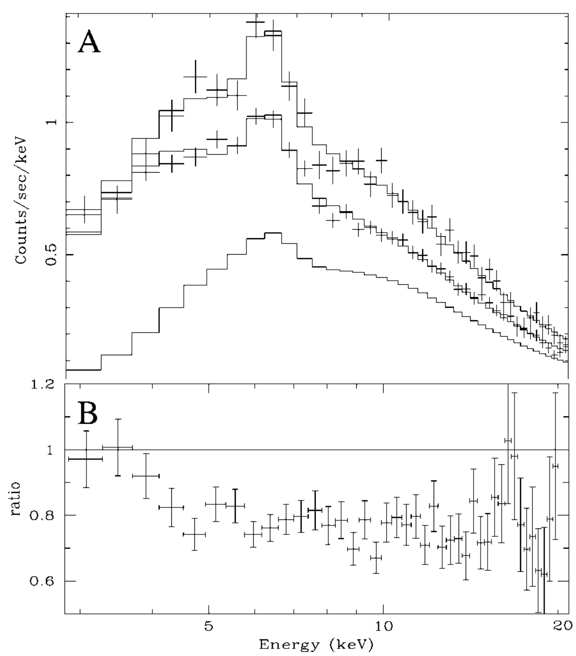

Fig. 2.—*Top*: *RXTE* spectra of NGC 4388. For comparison, we also plot the best-fit model of the *Chandra* observation performed 1 yr earlier, convolved with the response and effective area of the PCA and extrapolated from 10 to 20 keV for clarity. *Bottom*: Ratio of PCA-2 to PCA-1, showing greater variability at low energies. No change in N_H would give a flat line. [*See the electronic edition of the Journal for a color version of this figure.*]

Galactic N_H (2.5×10^{20} cm^{-2}; Murphy et al. 1996) is negligible for the PCA energy range. The total flux in the kiloparsec-scale X-ray nebula around NGC 4388 (Iwasawa et al. 2003) is also negligible (2.6×10^{-13} ergs cm^{-2} s^{-1}). The results are given in Table 1, together with fits to the same model, with the same minimum energy, for two unpublished observations from *XMM-Newton* and for six data sets from the literature. The measured N_H in the two PCA observations is $\sim 5 \times 10^{22}$ cm^{-2} and less than 0.9×10^{21} cm^{-2}, respectively (90% confidence). This rapid change between the two PCA observations in 4 hr is significant at the 3.2 σ; i.e., there is a 0.14% chance that the N_H-value is the same in the two PCA observations (Arnaud & Dorman 2003).

The PCA N_H-values are 1 and 2 orders of magnitude, respectively, lower than in all previous X-ray observations of this source. In particular the PCA-1 N_H is 13 σ smaller than that measured by *XMM-Newton* 5 months earlier (*XMM*-2; Table 1). The change in N_H in the 5 months between *XMM*-1 and *XMM*-2 is significant at the 11 σ level.) The contour plot of Figure 3 shows that the dramatic reduction in N_H is not due to a degeneracy between Γ and N_H that is sometimes encountered in X-ray spectra. Γ is flat ($\Gamma = 0.8$–0.9) in the PCA spectra compared with both most of the earlier observations and unobscured type 1 AGNs ($\Gamma \sim 1.8$; Nandra et al. 1997; Reynolds 1997; Perola et al. 2002). The *XMM*-1 observation (Table 1) also gave a flat Γ, yet it is heavily obscured, so a flat spectrum is not a property correlated with a low N_H. The small ($\sim 10''$) beam size of *XMM-Newton* (Jansen et al. 2001) effectively rules out the possibility that the flat PCA spectral slope is due to another source lying within the ~ 1 deg^2 PCA field of view. The high 2–10 keV flux in the BeppoSAX-1 observation demonstrates that a similarly high flux does not reduce the observed N_H. So we must be seeing bulk motion across our line of sight, as in Risaliti et al. (2002).

The N_H variation is robust against reasonable changes in the model: (1) adding a reflection component (PEXRAV model; Magdziarz & Zdziarski 1995) does not alter Γ or N_H. Even leaving all the parameters free, the best fit is obtained with a covering factor ($R = \Omega/2\pi$) $R = 0$. The 90% confidence upper limits are $R < 0.8$ for the first observation and $R < 0.2$ for the second one. Fixing R to these upper limits, we obtain column densities $N_{H1} \sim 2 \times 10^{21}$ cm^{-2} and $N_{H2} \sim 8 \times 10^{22}$ cm^{-2}. (2) Adding a soft component, of course, does change the fit dramatically, as this component affects only the lowest channels. For blackbody emission at typical soft excess temperatures of $kT \sim 0.3$–1 keV, the required 0.1–2 keV flux is 20 mcrab, or a luminosity of 5×10^{42} ergs s^{-1}. This luminosity causes no physical problems, although a 10^4 s variation requires an optically thick source (Elvis et al. 1991); a sphere of the implied area has a radius of only 10^{10} cm, 0.3 lt-s. However, such a large low-energy flux is not suggested by the lowest energy PCA bins that were omitted from the fit.

The χ^2 test prefers an emission line consistent with the 6.4 keV Fe-K line but broadened by $\sigma = 0.42^{+0.14}_{-0.2}$ keV (90% confidence), i.e., FWHM $= 2.38\,\sigma = 1.0$ keV, FWHM$/E = 0.15c$). A broad line would make an origin for the line in a parsec-scale torus unlikely and would argue for wind or accretion disk origin. The *XMM*-2 observation, however, using the higher spectral resolution CCD EPIC detectors, gives a lower Gaussian σ (73 ± 20 eV), although the line may be complex. The PCA-2–measured equivalent width (EW) of the line, ~500 eV, is stronger than normal for a type 1 Seyfert but less strong than can be found in Compton-thick AGNs (Levenson et al. 2002). Again *XMM*-2 gives a more normal EW (~200 eV) for an AGN that is not Compton-thick.

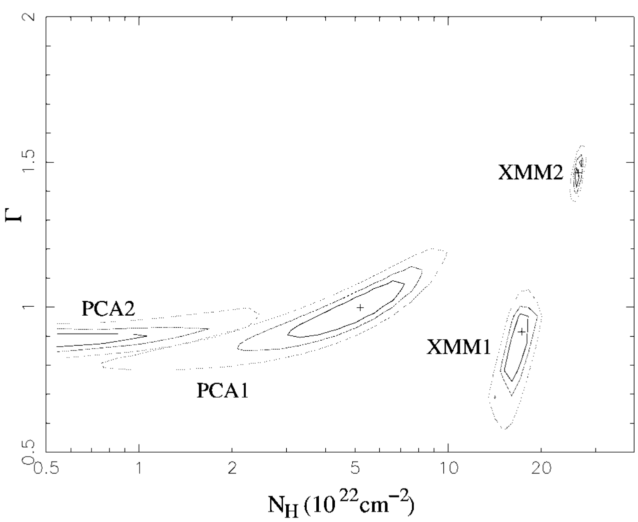

FIG. 3.—Photon index (Γ) vs. column density (N_H) contour plots (68%, 90%, and 99% confidence), derived here for the two PCA observations of 2003 May 2003 and the two *XMM-Newton* observations of 2002 July and December. [*See the electronic edition of the Journal for a color version of this figure.*]

The EW and σ of the PCA and *XMM*-1 are consistent but both disagree with the *XMM*-2 values.

3. DISCUSSION

We have found a factor of 100 decrease in the column density toward the normally almost Compton-thick ($\tau \sim 0.1$–0.3) type 2 AGN NGC 4388. This decrease certainly occurred in less than the 0.4 yr from the earlier *XMM-Newton* observation. The obscuring material in type 2 AGNs is thus in a highly dynamic state and warrants intensive monitoring. A few strongly Compton thick AGNs have become almost Compton thin on a timescale of 2.5–5.5 yr (Matt et al. 2003), but not on shorter timescales, and still with residual column densities of $\sim 10^{23}$ cm^{-2} even in the low absorption state, in three out of four cases. NGC 4388 is the only known case of an AGN in which a substantial X-ray opacity changes to an undetectable value ($\tau < 0.001$).

Moreover, it is likely that the decrease in obscuring column density coincided with the 2 day "flare" seen in the *RXTE* ASM, so that the flare is primarily an unveiling event. Without X-ray spectra through the rise of the ASM flux, however, we cannot be certain. Between the two PCA observations we saw evidence, at 3.2 σ, for a change of N_H in 4 hr.

The probable short timescale (either ~2 days or 4 hr) of the column density variations has strong implications for the location of the obscuring matter. Assuming that the absorption is due to clouds in Keplerian motion around the central source, and interpreting the 4 hr time lag between the two observations as the crossing time of a cloud, implies a distance from the center $R < 10^4 \rho_{10}^2 t_4^2 R_S$, where ρ_{10} is the density in units of 10^{10} cm^{-3}, R_S is the Schwarzschild radius, and t_4 is the timescale in units of 4 hr (Risaliti et al. 2002). If NGC 4388 has an Eddington ratio of 0.1, then the black hole mass is $\sim 10^6$–$10^7\,M_\odot$. Scaling from the *K*-band bulge magnitude gives a similar mass. This implies that the absorber is at a distance typical of the broad emission line region (BELR) "clouds" or smaller and is of similar density. Only if a high density ($\rho > 10^{12}$ cm^{-3}) is assumed can a parsec distant absorber produce changes on the observed timescale (Fig. 4). A similar conclusion applies to the Seyfert 1.5 galaxy NGC 4151, from the detection of a

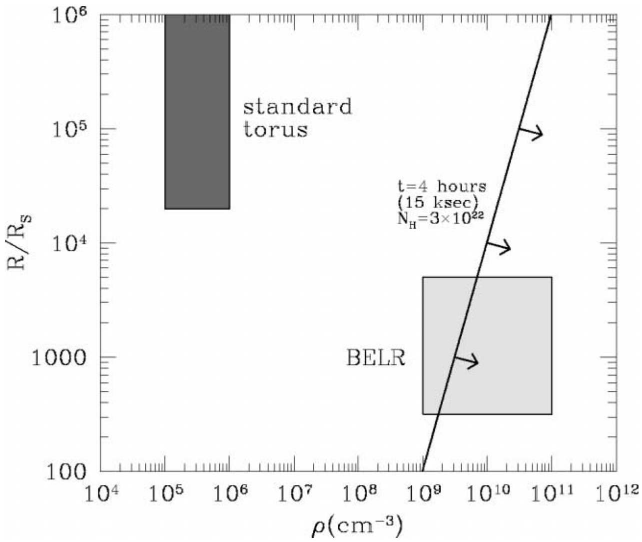

FIG. 4.—Distance (R/R_S) vs. density (ρ) plot for AGN X-ray absorbers. The "standard torus" of the unified model has a density $n < 10^6$ cm^{-3}. Variability of the absorber in 4 hr or less (*solid diagonal line*) rules out absorbers with such properties and is more compatible with the standard parameters of the BELRs. [*See the electronic edition of the Journal for a color version of this figure.*]

$\Delta(N_H) \sim 2 \times 10^{23}$ in a time interval of ~150 ks during a *BeppoSAX* observation (Puccetti et al. 2004).

This result is a challenge to the parsec scale usually attributed to the obscuring torus. For spherical isolated clouds, the high density implies small ($r_c \sim 10^{10}$ cm) cloud sizes: (1) the expansion time for a 100 K ($v_{\rm sound} \sim 1$ km s^{-1}) cloud from 10^{10} to 10^{11} cm is only 10^6 s, far shorter than the orbital time. But the large pressure needed to confine them ($p/k \sim 10^{14}$ K cm^{-3}) cannot be provided by self-gravity. (2) A hot confining medium would produce thermal emission much greater than the observed AGN bolometric luminosity (assuming a layer of 1 pc thickness, $L_{\rm gas} = 10^{48} T_7 n_7^2$ ergs s^{-1}, where T_7 and n_7 are the density and temperature in units of 10^7 K and 10^7 cm^{-3}, respectively (Rybicki & Lightman 1979). (3) The N_H through a confining medium would be $10^{25.5} n_7 d_{\rm pc}$ cm^{-2} $= 10\tau_{\rm es}$. So all continuum variations shorter than a few years would be smeared out by Thomson scattering, contrary to observations (Table 1). (4) Individual clouds would cover only a small fraction, ~10^{-6}, of the X-ray–emitting source, whose dimensions are greater than 10^{13} cm for a black hole of mass greater than $10^7\ M_\odot$. If hundreds of clouds are needed to cover the X-ray source, no N_H variation by more than a few percent can be observed with significant probability.

To produce large variations in N_H compatible with $\langle N_c \rangle \sim$ 5–10 needs clouds of a diameter within a factor of a few of the continuum source size. This implies a density of ~10^9 cm^{-3}. This is just compatible with a radius $R \sim$ few $\times$ $100R_S$ given a 4 hr variation (Fig. 4). If the absorbers are part of a wind crossing our line of sight (Elvis 2000), then sheetlike structures (Arav et al. 1998) become plausible, and this allows larger radii.

The great majority (>99%) of the obscuring *gas* in NGC 4388 occurs at small radii, and the most likely scenario is that BELRs are drifting across our line of sight in NGC 4388, leading to large changes in N_H. Similar behavior has been seen in some type 1 AGNs, involving an $N_H \sim 10^{23}$ cm^{-2} over ~100 days at the radius of the BELR (Lamer et al. 2003).

Since we have no simultaneous optical spectra, we do not know whether the bulk of the dust, which absorbs the optical and UV photons, lies on the same small scale. The closest that dust could be to the continuum is the sublimation radius (Barvainis 1993), which in NGC 4388 at ~10^{42} ergs s^{-1} (2–10 keV) is ~7×10^{16} cm (0.02 pc) or $2 \times 10^4 R_S(M_7)$ (Fig. 4). The dust-to-gas ratio in AGNs is typically a factor of 10 below the Milky Way value (Maccacaro et al. 1982; Maiolino et al. 2001), so that a separate dusty absorber is allowed. Unveiling events in type 2 AGNs, such as the one reported here for NGC 4388, put strong constraints on unified models for AGNs and seem to point to a different view of the obscuring torus.

This Letter used results provided by the ASM/*RXTE* teams at MIT and at the *RXTE* Science Operations Facility and Guest Observer Facility at NASA's GSFC. J. M. M. acknowledges the NSF. This work was partially supported by Chandra grant GO2-3122A.

REFERENCES

Antonucci, R. 1993, ARA&A, 31, 473
Arav, N., Barlow, T. A., Laor, A., Sargent, W. L. W., & Blandford, R. D. 1998, MNRAS, 297, 990
Arnaud, K., & Dorman, B. 2003, XSPEC 11.3 User Guide, http://heasarc.gsfc.nasa.gov/docs/xanadu/xspec/manual/manual.html
Barvainis, R. 1993, ApJ, 412, 513
Elvis, M. 2000, ApJ, 545, 63
Elvis, M., et al. 1991, ApJ, 378, 537
Forman, W., Schwarz, J., Jones, C., Liller, W., & Fabian, A. C. 1979, ApJ, 234, L27
Forster, K., Leighly, K. M., & Kay, L. E. 1999, ApJ, 523, 521
Hanson, C. G., Skinner, G. K., Eyles, C. J., & Willmore, A. P. 1990, MNRAS, 242, 262
Huchra, J. P., Wyatt, W. F., & Davis, M. 1982, AJ, 87, 1628
Iwasawa, K., Wilson, A. S., Fabian, A. C., & Young, A. J. 2003, MNRAS, 345, 369
Jansen, F., et al. 2001, A&A, 365, L1
Kartje, J. F., Königl, A., & Elitzur, M. 1999, ApJ, 513, 180
Khachikian, E. Y., & Weedman, D. W. 1974, ApJ, 192, 581
Krolik, J. H., & Begelman, M. C. 1988, ApJ, 329, 702
Lamer, G., Uttley, P., & McHardy, I. M. 2003, MNRAS, 342, L41
Levenson, N., et al. 2002, ApJ, 573, L81
Maccacaro, T., Perola, G. C., & Elvis, M. 1982, ApJ, 257, 47
Magdziarz, P., & Zdziarski, A. A. 1995, MNRAS, 273, 837
Maiolino, R., Marconi, A., Salvati, M., Risaliti, G., Severgnini, P., Oliva, E., La Franca, F., & Vanzi, L. 2001, A&A, 365, 28
Markowitz, A., et al. 2003, BAAS, 203, 63.03
Matt, G., Guainazzi, M., & Maiolino, R. 2003, MNRAS, 342, 422
Mulchaey, J. S., Koratkar, A., Ward, M. J., Wilson, A. S., Whittle, M., Antonucci, R. R. J., Kinney, A. L., & Hurt, T. 1994, ApJ, 436, 586
Murphy, E. M., Lockman, F. J., Laor, A., & Elvis, M. 1996, ApJS, 105, 369
Nandra, K., George, I. M., Mushotzky, R. F., Turner, T. J., & Yaqoob, T. 1997, ApJ, 476, 70
Perola, G. C., Matt, G., Cappi, M., Fiore, F., Guainazzi, M., Maraschi, L., Petrucci, P. O., & Piro, L. 2002, A&A, 389, 802
Pier, E. A., & Krolik, J. H. 1992, ApJ, 399, L23
———. 1993, ApJ, 418, 673
Puccetti, S., Risaliti, G., Fiore, F., Elvis, M., Nicastro, F., Perola, G. C., & Capalbi, M. 2004, Nucl. Phys. B, 132, 225
Remillard, R. A., & Levine, A. M. 1997, in All-Sky X-Ray Observations in the Next Decade, ed. M. Matsuoka & N. Kawai (Wako: Riken), 29
Reynolds, C. S. 1997, MNRAS, 286, 513
Risaliti, G. 2002, A&A, 386, 379
Risaliti, G., Elvis, M., & Nicastro, F. 2002, ApJ, 571, 234
Rybicki, G., & Lightman, A. P. 1979, Radiative Processes in Astrophysics (New York: Wiley)
Swank, J. H. 1998, in The Active X-ray Sky: Results from *BeppoSAX* and *RXTE*, ed. L. Scarsi, H. Bradt, P. Giommi, & F. Fiore (Amsterdam: Elsevier), 12
Urry, C. M., & Padovani, P. 1995, PASP, 107, 803